



HYPOKINETIC RIGID SYNDROME, IDIOPATHIC PARKINSON'S: A SMALL ACT OF CARING TO TURN A POTENTIAL LIFE

¹*Tanima Debnath Sarkar, ²John Anbumani Ganesan and ³P. Senthil Elango

¹Department of Zoology, Annamalai University.

²Department of Biochemistry and Biotechnology of Annamalai University, Chidambaram, Annamalainagar-608002, Tamil Nadu, India.

³Department of Zoology, M.V. Muthiah Government Arts College for Women, Dindigul. Tamil Nadu, India.

Article Received date: 01 December 2023

Article Revised date: 22 December 2023

Article Accepted date: 11 January 2024



*Corresponding Author: Tanima Debnath Sarkar

Department of Zoology, Annamalai University.

ABSTRACT

In Parkinson's disease (PD), the degeneration of the substantia nigra disrupts the nigrostriatal pathway, leading to a reduction in striatal dopamine levels and the emergence of PD symptoms. While dopamine itself faces challenges in crossing the blood-brain barrier, its precursor, levodopa, is capable of doing so. Levodopa undergoes absorption in the small bowel and is swiftly broken down by aromatic-L-amino-acid decarboxylase (AADC) and catechol-O-methyltransferase (COMT). Given that gastric AADC and COMT contribute to the degradation of levodopa, the drug is administered alongside inhibitors of AADC (such as carbidopa or benserazide). Additionally, inhibitors of COMT are anticipated to see clinical use. The specific location of the decarboxylation of exogenous levodopa to dopamine in the brain remains unknown, but a significant portion of striatal AADC is situated in the nerve terminals of nigrostriatal dopaminergic pathways. Dopamine, synthesized and stored a new terminals and subsequently released which stimulates postsynaptic dopamine receptors, mediating the antiparkinsonian effects of levodopa. Dopamine agonists, in contrast, act directly on postsynaptic dopamine receptors, eliminating the need for metabolic conversion, storage, and release. Parkinson disease protein7 (PARK7) or Protein deglycase (DJ-1) is a gene responsible for hereditary recessive Parkinson's disease (PD). The potential inhibition of monoamine oxidase B (MAO-B) getting from chalcone in human body by adenosine A_{2A} receptor (AA_{2A}R) antagonists has sparked interest in developing drugs that target both receptors. This dual-target approach holds promise for not only improving symptomatic relief but also potentially slowing the progression of Parkinson's disease (PD) by safeguarding against additional neurodegeneration.

KEYWORDS: Dopamine, nigrostriatal pathway, levodopa, amino acid decarboxylase, catechol-o-methyltransferase, L-amino-acid decarboxylase, dopaminergic pathways.

INTRODUCTION

The primary manifestations of Parkinson's disease arise primarily due to diminished or declining levels of dopamine, a neurotransmitter. This decline occurs when the cells responsible for dopamine production in the brain undergo degeneration. Dopamine serves a crucial role in transmitting messages to the brain region governing movement and coordination. Consequently, reduced dopamine levels can impede individuals' ability to regulate their movements. As dopamine levels continue to decrease, the symptoms progressively intensify.

Additionally, Parkinson's disease may encompass damage to the nerve endings that generate another

neurotransmitter, norepinephrine. Norepinephrine contributes in small functions such as blood circulation and other automatic bodily processes. Diminished levels of norepinephrine in Parkinson's disease may heighten the susceptibility to both motor and nonmotor symptoms.

The etiology of PD appears to intertwine with both environmental and genetic influences, with the onset of brain lesions potentially triggered by exposure to toxins and gene mutations. Several recognized mechanisms contribute to the manifestation of PD, encompassing α -synuclein aggregation, oxidative stress, ferroptosis, mitochondrial dysfunction, neuroinflammation, and gut dysbiosis. The intricate interplay among these molecular processes complicates the understanding of PD

pathogenesis and significantly hampers progress in drug development. Simultaneously, the intricate nature of PD, characterized by a lengthy latency period and complex mechanisms, poses significant hurdles in its diagnosis and detection, further impeding effective treatment.

BACKGROUND: PD is second to Alzheimer's disease as the most common age-related complex, idiopathic neurological disorder.^[1] In 1817, James Parkinson published his monograph titled *An Essay on the Shaking Palsy* which represents the first description of PD as a neurological disorder.^[44] Beginning with Jean-Martin Charcot, a succession of scientists contributed to the comprehensive description of the clinical range and anatomic pathological basis of PD, including motor, non-motor symptoms, the neuropathological changes in the substantia nigra (SN), Lewy bodies, and the role of dopamine.^[45,46] It is characterized by tremor, bradykinesia and muscle rigidity along with impaired gait, and posture.^[2-4] In addition, about half of the PD patients also exhibit frontostriatal-mediated executive dysfunction, including deficits in attention, speed of mental processing, verbal disturbances, impairment of working memory and impulsivity.^[5]



Figure 1: Exposures and environmental risk factors of Parkinson's diseases.

Due to loss of the substantia nigra pars compacta (SNpc), mitochondrial damage, energy failure, oxidative stress, excitotoxicity, protein misfolding and their aggregation, impairment of protein clearance pathways, cell-autonomous mechanisms and “prion-like protein infection” may be involved in the onset and progression of PD.^[3,6,7]

(i) Role of dopamine: The SNpc, a crucial component of the basal ganglia, is the primary brain region impacted by PD.^[8] Comprising mainly dopamine (DA)-secreting neurons, this area plays a pivotal role in regulating brain function. Dopamine, a vital monoamine, serves primarily as an inhibitory neurotransmitter. In a healthy brain, dopamine modulates the excitability of striatal neurons, crucial for coordinating body movements. However, in PD, degeneration of DA-producing neurons in the SNpc results in reduced dopamine levels.^[8,9] This deficiency diminishes the inhibition of striatal neuron activity, allowing them to become hyperactive. Consequently,

individuals with PD struggle to control their movements, manifesting as tremors, rigidity, and bradykinesia, characteristic motor symptoms of Parkinson's disease.^[3]

(ii) Role of serotonin: In addition to dopamine (DA), serotonin (5-HT) also assumes a significant role in the development of Parkinson's disease (PD), influencing various motor and non-motor symptoms such as tremor, cognition, depression, psychosis, and L-DOPA-induced dyskinesia.^[10] Observations in PD brains include a reduction in serotonin transporter (SERT)-immunoreactive axons in the prefrontal cortex (PFC), leading to decreased 5-HT immunoreactivity in median raphe neurons. Additionally, a decrease in PFC SERT binding capacity has been noted.^[11,12] PD patients exhibit approximately a 25% loss of serotonergic receptor (HT1A) at the median raphe nucleus, and this loss correlates with the severity of resting tremor, suggesting that 5-HT projections in the midbrain may be more pertinent to the initiation of PD tremor than the loss of nigrostriatal DA projections.^[13] Recent research has indicated that 5-HT turnover in the PFC could play a crucial role in executive dysfunction in the 1-methyl-4-phenyl-1,2,3,6-tetrahydropyridine (MPTP) model of PD.^[14] Furthermore, a substantial link between the decline in 5-HT and depression in PD has been established by several investigators.^[15]

(iii) Role of acetylcholine: The role of acetylcholine (ACh), crucial for cognition, is diminished in various neurological disorders, including PD and Alzheimer's disease (AD).^[16] The nucleus basalis of Meynert (nbM), a cholinergic-rich region within the basal forebrain subventricular area, exhibits significant cell clusters. Patients with PD, Lewy body dementia (LBD), AD, or other forms of dementia display diverse patterns of neuronal loss in the nbM, emphasizing the involvement of the cholinergic system in PD.^[16,17]

(iv) Role of GABA/Ca²⁺ system: Gamma-aminobutyric acid (GABA) is a neurotransmitter with inhibitory functions, directly regulating calcium (Ca⁺⁺) influx through GABAergic receptors and indirectly through astrocyte networks.^[18] The Ca⁺⁺/GABA mechanism contributes to stabilizing neuronal activity at both cellular and systemic levels. In PD, mitochondrial damage impairs the Ca⁺⁺ buffering system, leading to Ca⁺⁺ excitotoxicity and subsequent neuronal loss in the substantia nigra pars compacta (SNpc).^[19] GABA activity plays a crucial role in controlling Ca⁺⁺ buffering, and its disruption is implicated in PD pathology.^[20]

Approximately 80% of newly diagnosed PD patients exhibit abnormal olfaction, attributed to damage to DA-neurons in the olfactory bulbs.^[21] The functioning of DA-neurons in both the midbrain and olfactory system is regulated by the glial cell-derived neurotrophic factor (GDNF), which, in turn, is influenced by the Ca⁺⁺/GABA system. GDNF serves as a chemoattractant for GABAergic cells and a potent attractant for DA axons.

Neuroprotective effects of GDNF have been observed in PD animal models when administered to GABAergic neurons in the striatum, but not in the SNpc.^[22] This suggests that the breakdown of the GABA/Ca⁺⁺ system may play a role in DA-neuronal death in PD.^[23]

Mechanism of signaling path way of Parkinson’s disease: Mesencephalic neurons, the substantia nigra (SN) and ventral tegmental area (VTA) are synthesized by the catecholamine neurotransmitter predominant DA which is originated in the striatum, cortex, limbic system and hypothalamus. Dopamine engages with membrane

receptors from the seven-transmembrane domain G-protein coupled receptor family. Upon activation, these receptors initiate the generation of second messengers, influencing the activation or suppression of specific signaling pathways. Currently, five distinct subtypes of dopamine (DA) receptors have been identified across various species. Classification based on structural and pharmacological characteristics results in two main groups: the D1-like receptors, such as D1 and D5, which stimulate intracellular cAMP levels, and the D2-like receptors, including D2, D3, and D4, that inhibit intracellular cAMP levels.^[24-31]

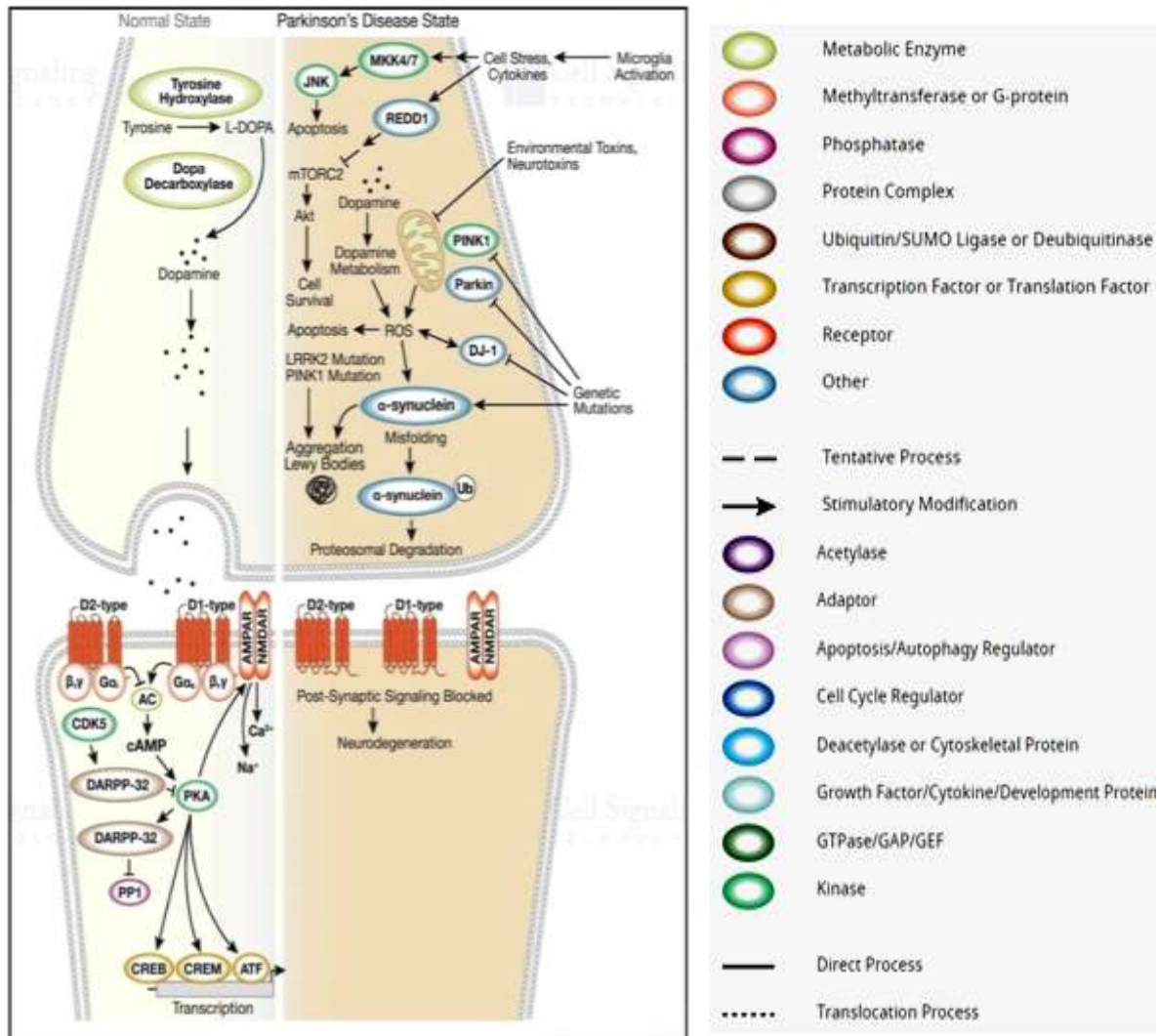
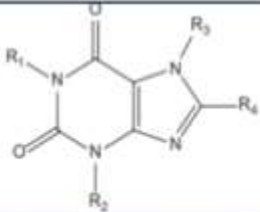


Figure 2: Signaling pathway diagrams of Parkinson’s disease.

MATERIALS AND METHODS

UniProt Database: The UniProt Knowledgebase (UniProtKB) serves as the primary repository for comprehensive protein information, offering precise, uniform, and detailed annotations. The FASTA sequence was acquired from the UniProt database, and the UniProt ID for the sequence is Q99497. The corresponding PDB ID was also obtained from the UniProt database.

Protein Data Bank: For the present study, crystal structures of human MAO-B (PDB code: 2V5Z)^[32] and human AA_{2A}R (PDB code: 3EML)^[33] were downloaded from the protein databank (www.rcsb.org/pdb). A set of 18 inhibitors [Table-1] that inhibit MAO-B and antagonize AA_{2A}R were taken from the literature^[34,35,36] and docked onto the active site of MAO-B and AA_{2A}R using AutoDock 4.2 (Release 4.2.2.1) program.

Table 1: The structures, Ki and pKi values for MAO-B inhibition and AA_{2A}R antagonism by 8-substituted caffeinyl analogs.^[37]


Compounds	R ₁	R ₂	R ₃	R ₄	MAO-B		AA _{2A} R	
					K _i ¹	pK _i	K _i ²	pK _i
1	Me	Me	Me	H	3.6 ^{1a}	2.44	22000 ²	4.66
2	Me	Me	Me	3-Chlorostyryl	0.235 ^{1a}	6.63	54 ²	7.28
3	Et	Et	Me	3,4-Dimethoxystyryl	17 ^{1a}	4.77	4.46 ²	8.35
4	Et	Et	H	3,4-Dimethoxystyryl	63 ^{1a}	4.20	23 ²	7.64
5	Me	Me	H	3,4-Dimethoxystyryl	6 ^{1a}	5.22	1100 ²	5.96
6	Me	Me	Me	3,4-Dimethoxystyryl	2.7 ^{1a}	5.57	197 ²	6.71
7	Me	Me	H	3-Nitrostyryl	9 ^{1a}	5.05	438 ²	6.36
8	Me	Me	Me	Styryl	3 ^{1a}	5.52	94 ²	7.03
9	Me	Me	H	Styryl	31 ^{1a}	4.51	291 ²	6.54
10	Me	Me	H	3-Fluorostyryl	1.9 ^{1a}	5.72	516 ²	6.29
11	Me	Me	Me	3-Nitrostyryl	0.16 ^{1a}	6.80	195 ²	6.71
12	Me	Me	Me	3-Fluorostyryl	0.4 ^{1a}	6.40	83 ²	7.08
13	Et	Et	Me	3,4-Methylenedioxytyryl	8 ^{1a}	5.10	6.1 ²	8.21
14	Me	Me	Me	4-phenylbutadien-1-yl	148.6 ^{1a}	6.83	153 ²	6.82
15	Me	Me	Me	4-(3-chlorophenyl)butadien-1-yl	42.1 ^{1a}	7.38	104 ²	6.98
16	Me	Me	Me	4-(3-bromophenyl)butadien-1-yl	17.2 ^{1a}	7.76	59.1 ²	7.23
17	Me	Me	Me	4-(3-fluorophenyl)butadien-1-yl	46.4 ^{1a}	7.33	114 ²	6.94
18	Me	Me	Et	4-phenylbutadien-1-yl	1712 ^{1a}	5.77	13.5 ²	7.87

MAO-B, monoamine oxidase B; AA_{2A}R, adenosine A_{2A} receptor; K_i¹, experimentally determined inhibition constant; pK_i, negative logarithm of K_i¹; Value given in nM; ² Values given in μM; ³ Values given in nM; ^{4,5,6,7,8,9,10,11,12,13,14,15,16,17,18} Experimental K_i taken from Refs. 15 and 18–24 respectively.

Molecular docking studies: The Lamarckian genetic algorithm approach was employed in conducting studies on flexible ligand docking.^[39] In AutoDock 4.2 docking experiments, ligand molecules were initially created in ChemBioDraw Ultra 12.0 and then transformed into their three-dimensional structures using ChemBio3D Ultra 12.0. Subsequently, energy minimization was performed through the PM3 method utilizing the MOPAC Ultra 2009 program.^[38] The resulting ligands, after preparation, served as input files for the AutoDock 4.2 software. The standard docking procedure was applied to a rigid protein and a flexible ligand with identified torsion angles, with 10 independent runs for each ligand. Caffeine itself at adenosine receptors.

A grid of 60, 60, and 60 points in the x, y, and z directions, respectively, was constructed, featuring a grid spacing of 0.375 Å. The calculation of the energetic map incorporated a distance-dependent function of the dielectric constant. Default settings were maintained for all other parameters. Post-docking, the best poses were scrutinized for hydrogen bonding/ π - π interactions, and root mean square deviation (RMSD) calculations were performed using Discovery Studio Visualizer 2.5.

The estimated free energy of ligand binding ($\Delta G_{\text{binding}}$, kcal/mol) was employed to calculate the inhibition constant (K_i) for each ligand. [Table-2]

Table 2.

	Safinamide+Monoamine oxidaseB	ZM241385+ AA _{2A} R
1.Binding energy	3.47	7.21
2.Ligand efficiency	0.16	0.29
3.Inhib constant	2.86	5.17
4.Intermol energy	5.56	9.3
5.Vdw_hb_desolv_energy	5.42	4.91
6.Electrostatic energy	0.14	4.39
7.Total internal	1.11	0.18
8.Torsional	2.09	2.09
9.Unbound energy	1.11	0.18

Calculation of physicochemical parameters: Absorption (% ABS) was calculated by: % ABS = 109 – [0.345 × topological polar surface area (TPSA)] according to the method of Zhao et al.^[40] TPSA,^[41]

miLogP, number of rotatable bonds, and violations of Lipinski's "Rule of Five"^[42] were calculated using Molinspiration online property calculation toolkit.^[43]

RESULTS AND DISCUSSION

The values of the inhibition constant (K_i) [Table-3] for 1, 2, 13, 14, and 17 were determined for MAO-B reported the standard inhibitors safinamide which clearly shows that the presence of the $-CF_3$ group as the R_1 substituent [at the meta (13) or para (14) position of the phenyl ring] significantly improves both the potency of the inhibition and the selectivity toward the MAO-B isoform with respect to unsubstituted chalcone. Otherwise, the insertion of the $-NO_2$ group as the R_2 substituent at the meta position (1) is detrimental to both MAO-B inhibition and the selectivity index (S.I.).

Particularly noteworthy is the heightened efficacy of compound 13, emerging as the most potent and

discerning inhibitor for MAO-B. Notably, its inhibition constant value ($K_i = 5.0$ nM) surpasses that of safinamide ($K_i = 17$ nM), exhibiting excellent selectivity (S.I. = 920 vs 4820 for safinamide). In contrast, derivative 17 displays lower potency ($K_i = 22$ nM) and diminished selectivity (S.I. = 594) compared to 13 in our experimental conditions. It's important to highlight that the K_i value reported in [Table 3] for 17 is lower than the literature values^[47,48] due to determination under distinct experimental buffer and temperature conditions. It is noteworthy that the 15–17 subseries was previously assessed on MAO-B, revealing lower inhibitory potency for both 15 and 16 in comparison to 17.^[47,48]

Table 3.

Compound	Chalcone	1	2	13	14	17 ^c	Safinamide ^d
MAO-B	56±6	400±80	71±11	5.0±0.5	14.6±0.1	21.9±2.3	17±4
S.I. ^b	260:1	5.5:1	35:1	920:1	630:1	594:1	4820:1

13 exhibits favorable drug-like properties and possesses good blood–brain barrier permeability, as outlined in Table-3. The more stable binding mode, termed binding mode b, is illustrated as the predominant interaction in MAO-B.^[51,52] These two binding modes in MAO-B may be attributed to the unique morphology of this isoform,

characterized by two similar sub cavities separated by the Ile199 and Tyr326 side chains. This phenomenon aligns with previously reported binding modes for other chalcone inhibitors. The docking scores for MAO-B were -10 kcal·mol⁻¹ for binding mode a and -11 kcal·mol⁻¹ for binding mode b.^[49,50]

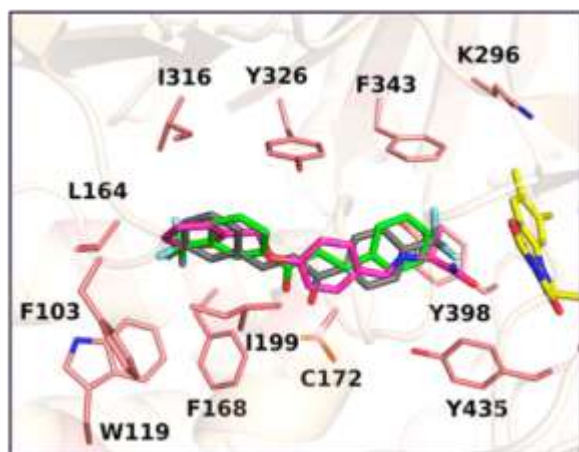


Figure 3: Superposition of MAO-B structures in 13s, 14, and safinamide (the latter represented atoms in magenta; PDB code 2V5Z).

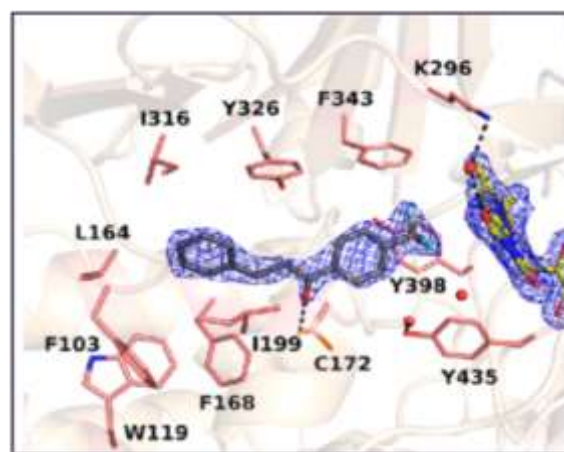


Figure 4: Binding MAOB (PDB complex with code-2V5Z) with ZM241385. with carbon.

Molecular docking: To assess the suitability of AutoDock 4.2 as a docking tool for the current study, the co-crystallized ligands (Safinamide and ZM241385 for 2V5Z.pdb and 3EML.pdb, respectively) were subjected to docking within the inhibitor-binding cavity (IBC) of human MAO-B and human AA_{2A}R. The resulting docked positions were compared to the crystal structure positions by calculating RMSD values, yielding 1.27 and 0.88 Å for MAO-B and AA_{2A}R, respectively.

Adhering to a widely accepted criterion, a docking tool is considered successful if the best-docked conformation of a ligand closely resembles the bound native ligand in the

experimental crystal structure. Following the validation method outlined in the literature^[53], a successful scoring function is defined as having an RMSD of the best-docked conformation ≤ 2.0 Å from the experimental one. In our study, both MAO-B and AA_{2A}R exhibited RMSD values within this threshold (as illustrated in Figure 5), affirming the validity of our docking methods. Consequently, AutoDock 4.2 is deemed reliable for the accurate docking of dual-target-directed drugs into the IBC of MAO-B and AA_{2A}R.

The active binding site of the co-crystallized AA_{2A}R antagonist, ZM241385, is defined by residues Leu-85,

Phe-168, Glu-169, Met-177, Trp-246, Leu-249, His-250, Asn-253, His-264, Leu-267, and Met-270.^[33] Our docking results, illustrated in Figure 2, provide a clear rationale for the observed low affinity of caffeine (compound 1) towards AA_{2A}R in experimental studies. Notably, none of the binding site residues interacted with caffeine, neither through hydrophobic nor hydrophilic interactions. However, in close proximity to the binding

cavity, caffeine formed a hydrogen bond with His-278. Intriguingly, our findings indicate that the xanthine nucleus assumes an orientation inside the binding cavity and engages in both hydrophobic and hydrophilic interactions when the C-8 position is substituted with (E)-styryl and 4-phenylbutadien-1-yl groups, rendering these compounds notably potent [Figure 7].

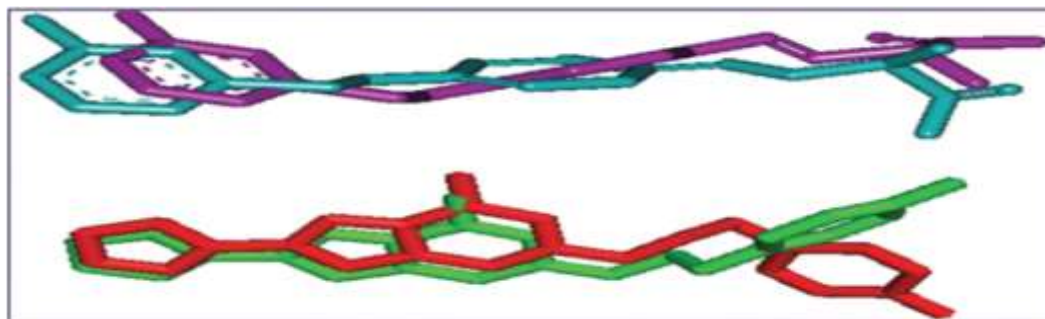


Figure 5: The validation of accuracy and performance of AutoDock 4.2. The docked safinamide (purple) and native safinamide (cyan) demonstrated a root mean square deviation of 1.27 Å, whereas the docked ZM241385 (red) and native ZM241385 (green) exhibited a root mean square deviation of 0.88 Å.

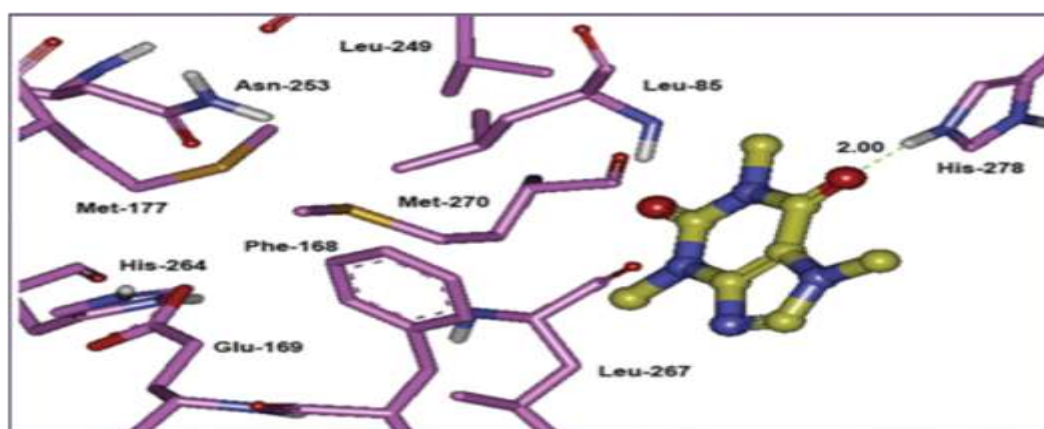


Figure 6: The lowest energy configuration of docking result of caffeine with binding pocket of human AA_{2A}R. The residues of binding pocket are shown as stick in pink color, and caffeine is presented as ball and stick style in yellow color. Dashed lines in green indicate H-bonds. Nitrogens are in blue and oxygens are in red.

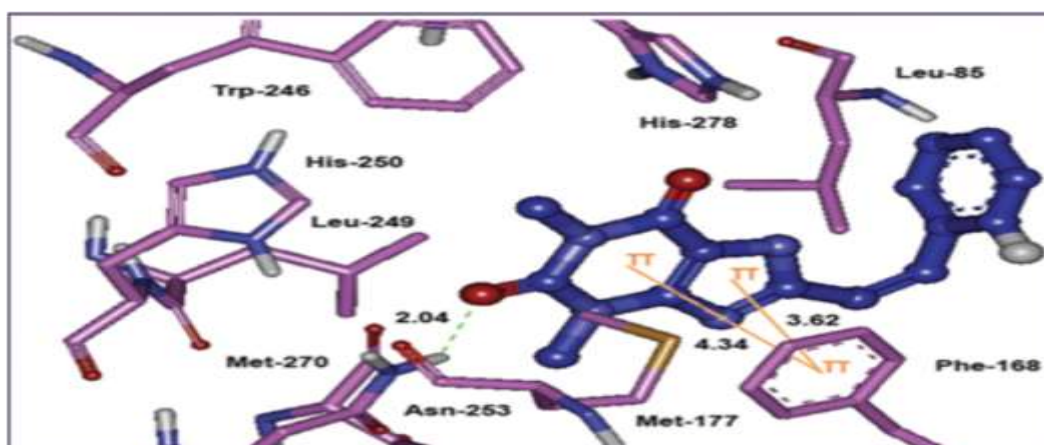


Figure 7: The lowest energy configuration of docking result of caffeinyl analog (Compound 10) with binding pocket of human AA_{2A}R. The residues of binding pocket are shown as stick in pink color while compound 10 is presented as ball and stick style in blue color. Dashed lines in green indicate H-bonds while π - π stacking interaction are shown as orange lines. Sulfur is presented in dark yellow and oxygens in red.

The bicyclic triazolotriazine core within ZM241385 establishes crucial interactions, including an aromatic stacking interaction with Phe-168^[55], an aliphatic hydrophobic interaction with Ile-274^[54,56], and a hydrogen bonding interaction with Asn-253.^[57,58,] Additionally, the bicyclic xanthine ring exhibits a π - π stacking interaction with the aromatic ring of Phe-168, while Asn-253 contributes to hydrophilic interaction through the formation of a hydrogen bond.

Moro et al. have reported that hydrophobic interactions involving Leu-249 also play a role in anchoring the bicyclic ring of ZM241385.^[59] In close proximity to Phe-168, the polar residue Glu-169 establishes a hydrogen bond with the oxygen atom of the 3,4-methylenedioxy group. A similar interaction is observed between the exocyclic amino group (N15 atom) linked to the bicyclic core of ZM241385.^[55,60]

Compounds 1–18, when docked, assumed a similar orientation within the IBC of both MAO-B and AA_{2A}R,

mimicking the interaction pattern observed with their respective native ligands safinamide and ZM241385, known to interact with MAO-B^[32] and AA_{2A}R.^[33]

The docking of caffeinyl derivatives into the IBC of human MAO-B highlighted specific interacting residues, including Pro-102, Leu-171, Cys-172, Ile-198, Ile-199, Gln-206, Ile-316, Tyr-326, Phe-343, Tyr-398, and Tyr-435, along with the isoalloxazine ring of FAD.^[61] A hydrophilic region adjacent to the flavin, crucial for substrate amine functionality recognition and directionality, was identified between Tyr-398 and Tyr-435.^[62]

This hydrophilic region plays a vital role in amine recognition, forming an aromatic cage along with the flavin. Furthermore, Gln-206, situated in this region, interacts by establishing a hydrogen bond with the native co-crystallized ligand safinamide.

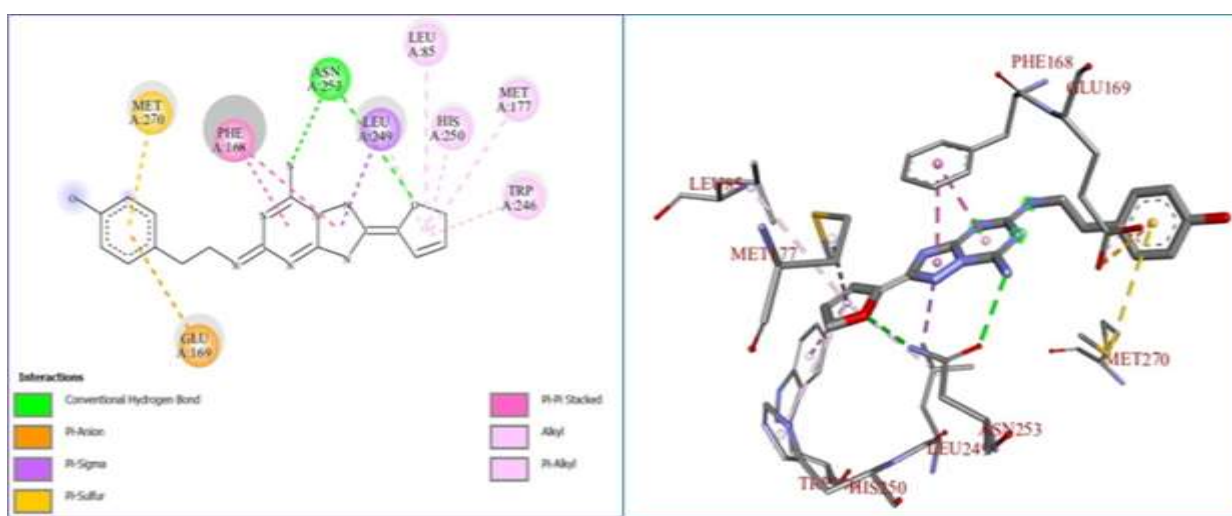


Figure-8

(a)

(b)

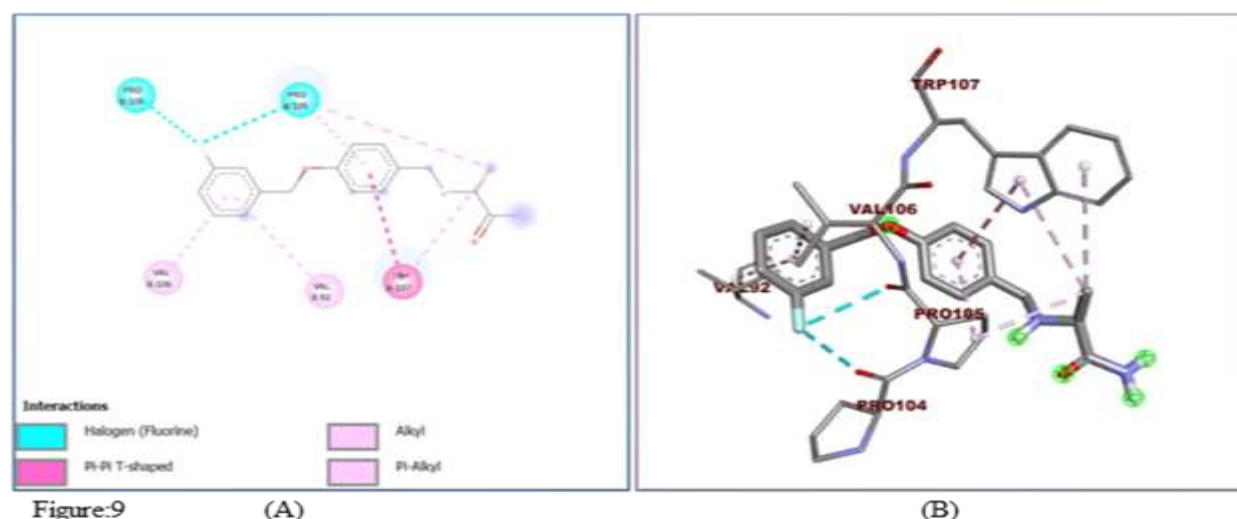
(a) 2D and (b) 3D structure of ZM241385+ AA_{2A}R docking.

Figure-9

(A)

(B)

(A) 2D and (B) 3D structure of Safinamide+Monoamine oxidaseB docking.

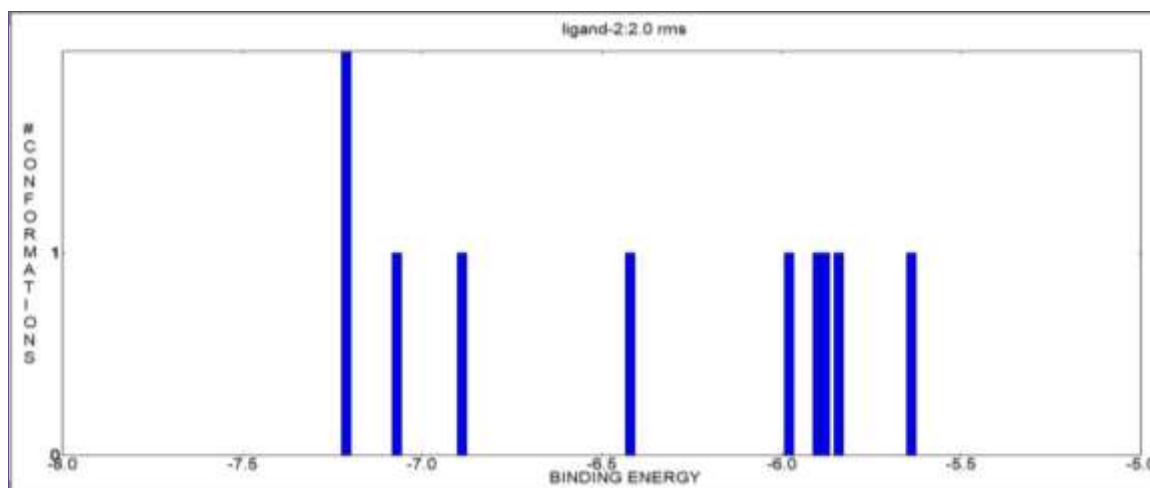


Figure 10: Binding energy graph of ZM241385+ AA_{2A}R docking.

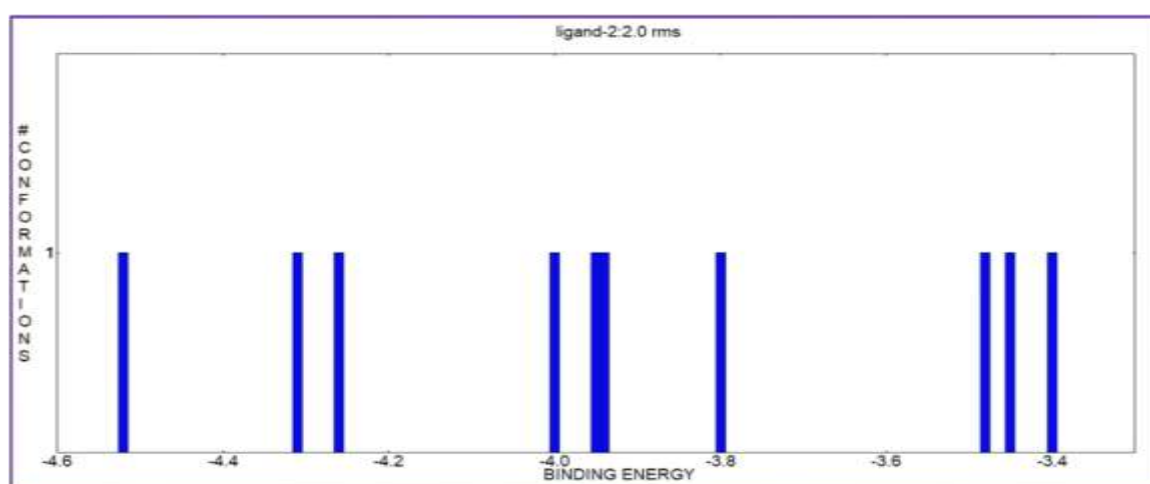


Figure 11: Binding energy graph of Safinamide+Monoamine oxidase B docking.

CONCLUSION

The review article highlights 13 as a highly promising chalcone derivative that merits consideration in the development of innovative MAO-B-selective inhibitors for addressing neurodegenerative diseases. The stem cell transplantation and gene therapy have treated a modern era. This biochemistry and bio informatics information has been acting a significant effective treatments for PD in the near horizon.

REFERENCES

1. Wright Willis A, Evanoff BA, Lian M, Criswell SR, Racette BA. Geographic and ethnic variation in Parkinson disease: a population-based study of US Medicare beneficiaries. *Neuroepidemiology*, 2010; 34(3): 143–51.
2. Jankovic J. Parkinson's disease: clinical features and diagnosis. *J Neurol Neurosurg Psychiatry*, 2008; 79(4): 368–76.
3. Alexander GE. Biology of Parkinson's disease: pathogenesis and pathophysiology of a multisystem neurodegenerative disorder. *Dialogues Clin Neurosci*, 2004; 6(3): 259–80.
4. Berardelli A, Rothwell JC, Thompson PD, Hallett M. Pathophysiology of bradykinesia in Parkinson's disease. *Brain*, 2001; 124(Pt 11): 2131–46.
5. Solari N, Bonito-Oliva A, Fisone G, Brambilla R. Understanding cognitive deficits in Parkinson's disease: lessons from preclinical animal models. *Learn Mem.*, 2013; 20(10): 592–600.
6. Davie CA. A review of Parkinson's disease. *Br Med Bull*, 2008; 86: 109–27.
7. Michel PP, Hirsch EC, Hunot S. Understanding dopaminergic cell death pathways in Parkinson disease. *Neuron*, 2016; 90(4): 675–91.
8. German DC, Manaye K, Smith WK, Woodward DJ, Saper CB. Midbrain dopaminergic cell loss in Parkinson's disease: computer visualization. *Ann Neurol*, 1989; 26(4): 507–14.
9. German DC, Manaye KF, Sonsalla PK, Brooks BA. Midbrain dopaminergic cell loss in Parkinson's disease and MPTP-induced parkinsonism: sparing of calbindin-D28k-containing cells. *Ann N Y Acad Sci.*, 1992; 648: 42–62.
10. Huot P, Sgambato-Faure V, Fox SH, McCreary AC. Serotonergic approaches in Parkinson's disease: translational perspectives, an update. *ACS Chem Neurosci*, 2017; 8(5): 973–86.

11. Guttman M, Boileau I, Warsh J, Saint-Cyr JA, Ginovart N, McCluskey T, Houle S, Wilson A, Mundo E, Rusjan P, et al. Brain serotonin transporter binding in nondepressed patients with Parkinson's disease. *Eur J Neurol.*, 2007; 14(5): 523–8.
12. Haapaniemi TH, Ahonen A, Torniaainen P, Sotaniemi KA, Myllyla VV. [123I]beta-CIT SPECT demonstrates decreased brain dopamine and serotonin transporter levels in untreated parkinsonian patients. *Mov Disord*, 2001; 16(1): 124–30.
13. Doder M, Rabiner EA, Turjanski N, Lees AJ, Brooks DJ. Study CWP: tremor in Parkinson's disease and serotonergic dysfunction: an 11C-WAY 100635 PET study. *Neurology*, 2003; 60(4): 601–5.
14. Maiti P, Gregg LC, McDonald MP. MPTP-induced executive dysfunction is associated with altered prefrontal serotonergic function. *Behav Brain Res.*, 2016; 298(Pt B): 192–201.
15. Tan SK, Hartung H, Sharp T, Temel Y. Serotonin-dependent depression in Parkinson's disease: a role for the subthalamic nucleus? *Neuropharmacology*, 2011; 61(3): 387–99
16. Tagliavini F, Pilleri G. Basal nucleus of Meynert. a neuropathological study in Alzheimer's disease, simple senile dementia, Pick's disease and Huntington's chorea. *J Neurol Sci.*, 1983; 62(1–3): 243–60.
17. Liu AK, Chang RC, Pearce RK, Gentleman SM. Nucleus basalis of Meynert revisited: anatomy, history and differential involvement in Alzheimer's and Parkinson's disease. *Acta Neuropathol*, 2015; 129(4): 527–40.
18. Allaman I, Belanger M, Magistretti PJ. Astrocyte-neuron metabolic relationships: for better and for worse. *Trends Neurosci*, 2011; 34(2): 76–87.
19. Hurley MJ, Brandon B, Gentleman SM, Dexter DT. Parkinson's disease is associated with altered expression of CaV1 channels and calcium-binding proteins. *Brain*, 2013; 136(Pt 7): 2077–97.
20. Glass CK, Saijo K, Winner B, Marchetto MC, Gage FH. Mechanisms underlying inflammation in neurodegeneration. *Cell.*, 2010; 140(6): 918–34.
21. Stefanis L. Alpha-Synuclein in Parkinson's disease. *Cold Spring Harb Perspect Med.*, 2012; 2(2): a009399.
22. Ibanez CF, Andressoo JO. Biology of GDNF and its receptors - relevance for disorders of the central nervous system. *Neurobiol Dis.*, 2017; 97(Pt B): 80–9.
23. Blaszczyk JW. Parkinson's disease and neurodegeneration: GABA-collapse hypothesis. *Front Neurosci*, 2016; 10: 269.
24. Dearry, A., Gingrich, J. A., Falardeau, P., Fremeau, R. T. Jr., Bates, M. D., et al. Molecular cloning and expression of the gene for a human D1 dopamine receptor. *Nature*, 1990; 347: 72–76. doi: 10.1038/347072a0
25. Dal Toso, R., Sommer, B., Ewert, M., Herb, A., Pritchett, D. B., Bach, A., et al. The dopamine D2 receptor: two molecular forms generated by alternative splicing. *EMBO J.*, 1989; 8: 4025–4034.
26. Zhou, Q. Y., Grandy, D. K., Thambi, L., Kushner, J. A., Van Tol, H. H., Cone, R., et al. Cloning and expression of human and rat D1 dopamine receptors. *Nature.*, 1990; 347: 76–80. doi: 10.1038/347076a0.
27. Grandy, D. K., Zhang, Y. A., Bouvier, C., Zhou, Q. Y., Johnson, R. A., Allen, L., et al. Multiple human D5 dopamine receptor genes: a functional receptor and two pseudogenes. *Proc. Natl. Acad. Sci. U.S.A.*, 1991; 88: 9175–9179. doi: 10.1073/pnas.88.20.9175.
28. Sunahara, R. K., Guan, H. C., O'Dowd, B. F., Seeman, P., Laurier, L. G., Ng, G., et al. Cloning of the gene for a human dopamine D5 receptor with higher affinity for dopamine than D1. *Nature*, 1991; 350: 614–619. doi: 10.1038/350614a0.
29. Sokoloff, P., Giros, B., Martres, M. P., Bouthenet M. L., and Schwartz, J. C. Molecular cloning and characterization of a novel dopamine receptor (D3) as a target for neuroleptics. *Nature*, 1990; 347: 146–151. doi: 10.1038/347146a0.
30. Van Tol, H. H., Bunzow, J. R., Guan, H. C., Sunahara, R. K., Seeman, P., Niznik, H. B., et al. Cloning of the gene for a human dopamine D4 receptor with high affinity for the antipsychotic clozapine. *Nature*, 1991; 350: 610–614. doi: 10.1038/350610a0.
31. Bunzow, J. R., Van Tol, H. H., Grandy, D. K., Albert, P., Salon, J., Christie, M., et al. Cloning and expression of a rat D2 dopamine receptor cDNA. *Nature*, 1988; 336: 783–787. doi: 10.1038/336783a0.
32. Binda C, Wang J, Pisani L, Caccia C, Carotti A, Salvati P, et al. Structure of human monoamine oxidase B, a drug target for the treatment of neurological disorders. *J Med Chem.*, 2007; 50: 5848-52.
33. Jaakola VP, Griffith MT, Hanson MA Cherezov V, Chien YE, Lane JR, et al. The 2.6 angstrom crystal structure of a human A2A adenosine receptor bound to an antagonist. *Science*, 2008; 322: 1211-7.
34. Cheng YC, Prusoff WH. Relationship between the inhibition constant (K_i) and the concentration of inhibitor which causes 50 per cent inhibition (I_{50}) of an enzymatic reaction. *Biochem Pharmacol*, 1973; 22: 3099-108.
35. Petzer JP, Castagnoli N, Schwarzschild MA, Chen J, Schyf CJ. Dual target- directed drugs that block monoamine oxidase B and adenosine A2A receptors for Parkinson's disease. *Neurotherapeutics*, 2009; 6: 141-51.
36. Muller CE, Geis U, Hipp J, Schobert U, Frobenius W, Pawlowski M, et al. Synthesis and structure-activity relationship of 3,7-dimethyl-1-propargylxanthine derivatives, A2A-selective adenosine receptor antagonists. *J Med Chem.*, 1997; 40: 4396-405.

37. Azam, F., Madi, A. M., & Ali, H. I. Molecular docking and prediction of pharmacokinetic properties of dual mechanism drugs that block MAO-B and adenosine A2A receptors for the treatment of Parkinson's disease. *Journal of Young Pharmacists*, 2012; 4(3): 184-192.
38. Stewart JJ. Stewart Computational Chemistry, Version 9.03CS. MOPAC 2009. Available from: <http://OpenMOPAC.net>.
39. Morris GM, Goodsell DS, Halliday RS, Huey R, Hart WE, Belew RK, et al. Automated docking using a Lamarckian genetic algorithm and an empirical binding free energy function. *J Comput Chem.*, 1998; 19: 1639-62.
40. Zhao Y, Abraham MH, Lee J, Hersey A, Luscombe NC, Beck G, et al. Rate-limited steps of human oral absorption and QSAR studies. *Pharm Res.*, 2002; 19: 1446-57.
41. Ertl P, Rohde B, Selzer P. Fast calculation of molecular polar surface area as a sum of fragment-based contributions and its application to the prediction of drug transport properties. *J Med Chem.*, 2000; 43: 3714-7.
42. Lipinski CA, Lombardo L, Dominy BW, Feeney PJ. Experimental and computational approaches to estimate solubility and permeability in drug discovery and development settings. *Adv Drug Deliv Rev.*, 2001; 46: 3-26.
43. Molinspiration Cheminformatics, Bratislava, Slovak Republic. Available from: <http://www.molinspiration.com/services/properties.html>. [Last Accessed on 2010 Apr 22].
44. Parkinson, J. An essay on the shaking palsy. 1817. *J. Neuropsychiatry Clin. Neurosci*, 2002; 14: 223-236.
45. Charcot, J. M. Lecons sur, les maladies du système nerveux, (Lecrosnier et Babé, 1886; 1.
46. Przedborski, S. The two-century journey of Parkinson disease research. *Nat. Rev. Neurosci*, 2017; 18: 251-259.
47. Choi, J. W.; Jang, B. K.; Cho, N.-c.; Park, J.-H.; Yeon, S. K.; Ju, E. J.; Lee, Y. S.; Han, G.; Pae, A. N.; Kim, D. J.; Park, K. D. Synthesis of a series of unsaturated ketone derivatives as selective and reversible monoamine oxidase inhibitors. *Bioorg. Med. Chem.*, 2015; 23: 6486- 6496.
48. Mathew, B.; Mathew, G. E.; Ucar, G.; Joy, M.; Nafna, E. K.; Lohidakshan, K. K.; Suresh, J. Monoamine oxidase inhibitory activity of methoxy-substituted chalcones. *Int. J. Biol. Macromol*, 2017; 104: 1321-1329.
49. Shalaby, R.; Petzer, J. P.; Petzer, A.; Ashraf, U. M.; Atari, E.; Alasmari, F.; Kumarasamy, S.; Sari, Y.; Khalil, A. SAR and molecular mechanism studies of monoamine oxidase inhibition by selected chalcone analogs. *J. Enzyme Inhib. Med. Chem.*, 2019; 34: 863-876.
50. Hammuda, A.; Shalaby, R.; Rovida, S.; Edmondson, D. E.; Binda, C.; Khalil, A. Design and synthesis of novel chalcones as potent selective monoamine oxidase-B inhibitors. *Eur. J. Med. Chem.*, 2016; 114: 162-169.
51. Binda, C.; Wang, J.; Pisani, L.; Caccia, C.; Carotti, A.; Salvati, P.; Edmondson, D. E.; Mattevi, A. Structures of human monoamine oxidase B Complexes with Selective noncovalent inhibitors: safinamide and coumarin analogs. *J. Med. Chem.*, 2007; 50: 5848-5852.
52. Son, S.-Y.; Ma, J.; Kondou, Y.; Yoshimura, M.; Yamashita, E.; Tsukahara, T. Structure of human monoamine oxidase A at 2.2-Å resolution: the control of opening the entry for substrates/inhibitors. *Proc. Natl. Acad. Sci. U. S. A.*, 2008; 105: 5739-5744.
53. Wang R, Lu Y, Wang S. Comparative evaluation of 11 scoring functions for molecular docking. *J Med Chem.*, 2003; 46: 2287-303.
54. Schwarzschild MA, Agnati L, Fuxe K, Chen JF, Morelli M. Targeting adenosine A2A receptors in Parkinson's disease. *Trends Neurosci*, 2006; 29: 647-54.
55. Sawynok J, Liu XJ. Adenosine in the spinal cord and periphery: Release and regulation of pain. *Prog Neurobiol*, 2003; 69: 313-40.
56. Yuzlenko O, Kiec-Kononowicz K. Molecular modeling of A1 and A2A adenosine receptors: Comparison of rhodopsin- and β_2 -adrenergicbased homology models through the docking studies. *J Comput Chem.*, 2008; 30: 14-32.
57. Shi Y, Liu X, Gebremedhin D, Falck JR, Harder DR, Koehler RC. Interaction of mechanisms involving epoxyeicosatrienoic acids, adenosine receptors, and metabotropic glutamate receptors in neurovascular coupling in rat whisker barrel cortex. *J Cereb Blood Flow Metab.*, 2008; 28: 111-25.
58. Kim J, Wess J, Van-Rhee AM, Schoneberg T, Jacobson KA. Site-directed mutagenesis identifies residues involved in ligand recognition in the human A2a adenosine receptor. *J Biol Chem.*, 1995; 270: 13987-97.
59. Moro S, Deflorian F, Spalluto G, Pastorin G, Cacciari B, Kim SK, et al. Demystifying the three dimensional structure of G protein-coupled receptors (GPCRs) with the aid of molecular modeling. *Chem Commun*, 2003; 24: 2949-56.
60. Hanson MA, Cherezov V, Griffith MT, Roth CB, Jaakola VP, Chien EY, et al. A specific cholesterol binding site is established by the 2.8 Å structure of the human beta2-adrenergic receptor. *Structure*, 2008; 16: 897-905.
62. De Colibus L, Li M, Binda C, Lustig A, Edmondson DE, Mattevi A. Threedimensional structure of human monoamine oxidase A (MAO A): Relation to the structures of rat MAO A and human MAO B. *Proc Natl Acad Sci U S A.*, 2005; 102: 12684-9.
63. Binda C, Li M, Hubalek F, Restelli N, Edmondson DE, Mattevi A. Insights into the mode of inhibition of human mitochondrial monoamine oxidase B from high-resolution crystal structures. *Proc Natl Acad Sci U S A.*, 2003; 100: 9750-5.